OXFORD

Potential for on-grid hybrid renewable energy in a humid subtropical climatic zone: technological, economic, and environmental aspects

Tao Hai[1,2,3,4], Hussein A. Jaffar[5,*] (ID), Hayder Oleiwi Shami[6,7], Ameer H. Al-Rubaye[8],
Husam Rajab[9,10], Rand Otbah Farqad[11], Abbas Hameed Abdul Hussein[12],
Wesam Abed AL Hassan Alhaidry[13], Ameer Hassan Idan[14], Narinderjit Singh Sawaran Singh[3]

[1]School of Information and Artificial Intelligence, Nanchang Institute of Science & Technology, Nanchang 330108, China
[2]School of Computer and Information, Qiannan Normal University for Nationalities, Duyun, Guizhou 558000, China
[3]Faculty of Data Science and Information Technology, INTI International University, 71800, Malaysia
[4]Artificial Intelligence Research Center (AIRC), Ajman University, P.O. Box 346, Ajman, UAE
[5]Air Conditioning Engineering Department, Faculty of Engineering, University of Warith Alanbiyaa, Karbala, Iraq
[6]Department of Accounting, Al-Amarah University College, Maysan, Iraq
[7]College of Administration and Economics, Department of Economics, University of Misan, Iraq
[8]Department of Petroleum Engineering, Al-Kitab University, Altun Kupri, Iraq
[9]College of Engineering Department of Mechanical Engineering, Najran University, King Abdulaziz Road, P.O. Box 1988, Najran, Kingdom of Saudi Arabia
[10]College of Engineering, Mechanical Engineering Department, Alasala University, King Fahad Bin Abdulaziz Rd., P.O. Box 12666 Amanah, 31483 Dammam, Kingdom of Saudi Arabia
[11]College of Dentistry, Alnoor University, Mosul, Iraq
[12]Ahl Al Bayt University, Kerbala, Iraq
[13]College of Technical Engineering, National University of Science and Technology, Dhi Qar 64001, Iraq
[14]Al-Zahrawi University College, Karbala, Iraq

*Corresponding author. Air Conditioning Engineering Department, Faculty of Engineering, University of Warith Alanbiyaa, Karbala, Iraq.
Email: hussein.a.j@uowa.edu.iq

Abstract

China's abundant natural resources reveal inconsistencies in economics, environment, and society. Renewable energy sources can reduce environmental pollutants and mitigate greenhouse gas emissions. Using HOMER software, Zhanjiang City, Guangdong Province, China, optimizes the economic, environmental, and technological aspects of creating an off-grid hybrid power system for 100 houses. According to the results, the most economically feasible photovoltaic (PV)–wind turbine (WT)–grid hybrid system is made up of one WT, 25.55 kW converters, and 80 kW PV panels. Its total net present cost (NPC) is \$494 119, and its cost of energy (COE) is \$0.043/kWh. However, because it has the greatest operation expenses, the PV–grid hybrid configuration has the highest NPC of \$687 906 and COE of \$0.068/kWh. Furthermore, according to the technical analysis's findings, WT contributed 49.2% of the overall power generation, equivalent to \$357 694/kWh. The optimal WT/PV/grid configuration, which is the suggested configuration, has the lowest yearly emissions of carbon dioxide (174 236 kg/year), whereas the PV–grid configuration has the highest carbon dioxide emissions (246 769 kg/year). The results of the sensitivity evaluation's findings demonstrate that the COE and NPC amounts for the ideal configuration decline as solar irradiation and wind velocity increase. To clarify, raising the system's velocity of wind or radiation from the sun can make it more economically viable. It may be concluded that the WT–PV–grid hybrid configuration is the more environmentally friendly and economical technology. Zhanjiang, China, has the potential to develop a sustainable alternative energy system combining WT and biomass power generation, but factors like fuel limitations and energy consumption must be considered.

Keywords: technological and economic potential; environmental; wind power; solar photovoltaic; hybrid renewable source; HOMER software

1 Introduction

The inherent inconsistencies within the fields of economics, environment, and society are becoming apparent in the parts of China that possess abundant natural resources. Utilizing renewable sources of energy can effectively reduce pollutants in the environment and mitigate greenhouse gas emissions [1, 2]. The two main clean energy-generating technologies, solar and wind power, are gradually replacing traditional energy generation, setting a trend in energy consumption [3, 4]. Various hybrid alternative energy systems are considered effective

methods of creating clean power, which can significantly reduce environmental pollution [5, 6]. Hybrid energy production utilizing wind and photovoltaic (PV) power generation has experienced a surge in popularity in recent years [7, 8]. Several countries view the advancement of renewable energy power generation as a key objective of their national policies and have allocated substantial funds toward this program [9, 10]. Examining the technological and economic consequences of hybrid environmentally friendly energy production is crucial for promoting the adoption and utilization of these

Table 1. An overview of comparative research on the use of economic and technological analysis for hybrid green power

System	Grid	Load type	Location	Reference
PV/WT/battery	Stand-alone	Residential	China	[13]
WT/DG/PV/battery	Stand-alone	Residential	China	[14]
DG/PV/battery	On-grid	Residential	Bangladesh	[15]
WT/PV/DG/FC/battery	Stand-alone	Residential	Iran	[16]
WT/PV/DG/FC/battery	Stand-alone	Educational	India	[17]
PV/DG/FC/electrolyzer/HT/battery	On-grid	Health clinic	Saudi Arabia	[18]
PV/FC/DG/HT/electrolyzer/battery	On-grid	Hospital	Malaysia	[19]
WT/PV/DG/battery	Stand-alone	Residential	Australia	[20]
PV/DG/Hydro/battery	Stand-alone	Residential	India	[21]
PV/WT/DG/battery	Stand-alone	Residential	India	[22]
WT/DG/PV/battery	Stand-alone	Residential	India	[23]
PV/WT/DG/Boiler/electrolyzer/battery	Stand-alone	Residential	Iran	[24]
DG/PV/battery/flywheel	Stand-alone	Residential	Saudi Arabia	[25]
WT/DG/PV/battery	On-grid	Residential	Iran	[26]
WT/BG/DG/PV/battery	Stand-alone	Residential	Iran	[27]
PV/BG/FC/battery/electrolyzer	Stand-alone	Residential	Cameroon	[28]
PV/WT/Diesel/battery	On-grid	Residential	Iran	[29]
WT/BG/DG/battery	Stand-alone	industrial	Iran	[30]
WT/PV/battery	On-grid	Residential	China	[31]
WT/BG/ PV/battery	On-grid	Residential	India	[32]
PV/DG/WT/battery/electrolyzer	Stand-alone	Residential	Bangladesh	[33]
PV/diesel/battery	Stand-alone	Residential	China	[34]

systems [11, 12]. Hybrid energy-generating systems that combine wind and PV power generation have gained widespread acceptance in recent times for their techno-economic evaluations. Table 1 presents many research projects that utilize HOMER software to improve the technical, economical, and ecological evaluations of hybrid clean energy sources.

Zhanjiang, China, has the potential to develop an alternative energy system combining wind turbine (WT) power and biomass power generation. This sustainable and environmentally friendly option could provide affordable, dependable, and affordable urban electrification. There have not been many studies on grid-connected generating systems in China's mild subtropical humid climate zone in terms of technology, economics, and the environment, according to the literature review previously discussed (Table 1). There is little research on building a grid-connected hybrid setup in slightly humid subtropical climate zones utilizing the multiyear model provided by HOMER software. The main goal of this study is to examine novel applications of on-grid hybrid green energy sources, which integrate solar PV cells with WTs, in a moderately humid subtropical climate zone.

This study aimed to assess the technical and financial feasibility of the on-grid arrangement in the moderately humid subtropical environment of Zhanjiang City using the HOMER simulation tool. Below is an explanation of the paper's structure:

The investigation's approach is described in the second part. The results are given and then discussed in the third part. In the last part of the investigation, the conclusions are provided.

2 Materials and methods
2.1 Explain the area being examined
Zhanjiang is an important port city with 1.6 million inhabitants in western Guangdong Province, China (21°13.1′N, 110°20.8′E). Fig. 1 depicts the geographical position of Zhanjiang [35].

2.2 Resource data
Fig. 2 depicts the mean monthly global horizontal irradiance (GHI) and clearness index (CI) data for Zhanjiang port city (July 1983 to June 2005) taken from NASA's Prediction of International Energy Resources database. As can be observed, Zhanjiang has an annual average GHI of 3.91 kWh/m^2/day and a CI of 0.421. Fig. 3 depicts the mean monthly wind velocity at a height of 50 m above the Earth's surface (January 1984 to December 2013) in the city of Zhanjiang. As can be observed, the mean monthly wind velocity in Zhanjiang is 5.73 m/s. Fig. 4 illustrates that the mean monthly temperature of the air in Zhanjiang port is 23.65°C.

2.3 Load data
The study examines the energy usage in residential properties within a hypothetical small community comprising 100 dwellings situated in Zhanjiang city. The domestic appliances under consideration encompass electric lights, air conditioners, TV sets, refrigerators, washing machines, rice cookers, and other similar devices [36]. Figs 5 and 6 depict the load patterns of the district in Zhanjiang city, showing the monthly and hourly profiles, respectively. The community has a total annual energy requirement of 1603 kWh/day, with a peak load demand of 340.48 kW.

2.4 Configuration and components of a hybrid configuration
This section provides a detailed analysis of the configuration and components of a hybrid configuration. The hybrid PV–wind turbine system being considered consists of PV modules, a WT, and converters, as shown in Fig. 7. The WT is connected via an alternating current bus, while the PV modules are connected via a direct current bus. An AC/DC converter establishes a connection between the alternating current bus and the direct current bus.

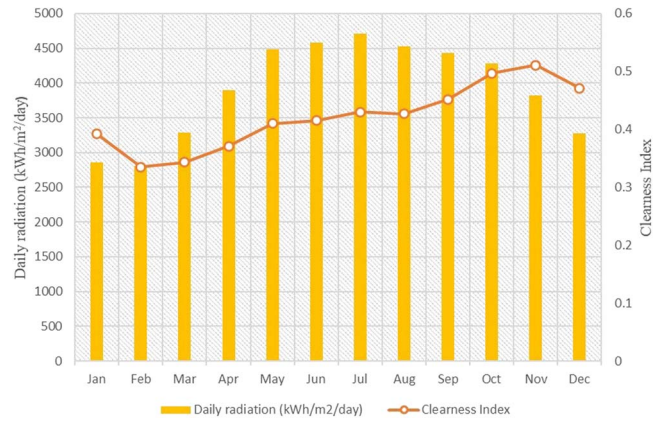Figure 1. Map of Zhanjiang harbor city, China [35].

Figure 2. Monthly data on average CI and GHI for the port city of Zhanjiang.

Figure 3. Monthly average wind speeds at a height of 50 m at Zhanjiang port are collected consistently every month of the year.

Figure 4. Average monthly average temperature for Zhanjiang city.
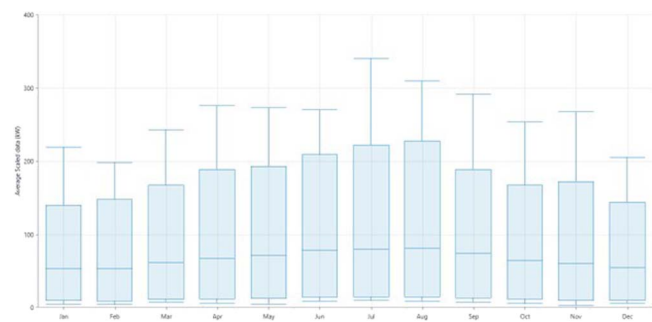
Figure 5. The load profile of Zhanjiang city on a monthly basis.

2.4.1 PV array

The simulation utilizes Jinko Solar 300 W monocrystalline silicon cells. The cells demonstrate a 13% efficiency under typical test settings. The PV's capacity is maximized using the HOMER optimizer. 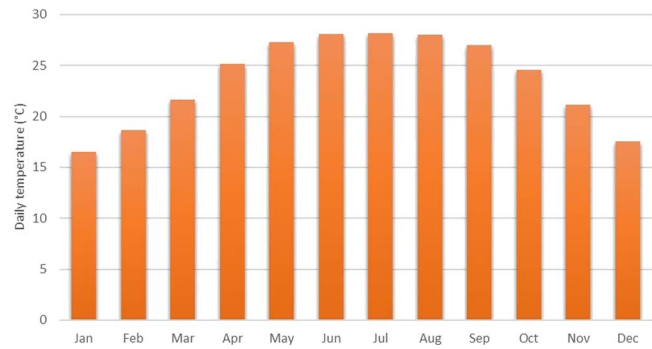The research assesses how the ambient temperature impacts the efficiency of solar panels. Specifically, the study analyzes how temperature affects both the output power and the nominal operating cell temperature. The resultant values are −0.439%/°C and 46.7°C, respectively. The power generated by the PV panels, accounting for temperature effects, is calculated using a specific formula [37]:

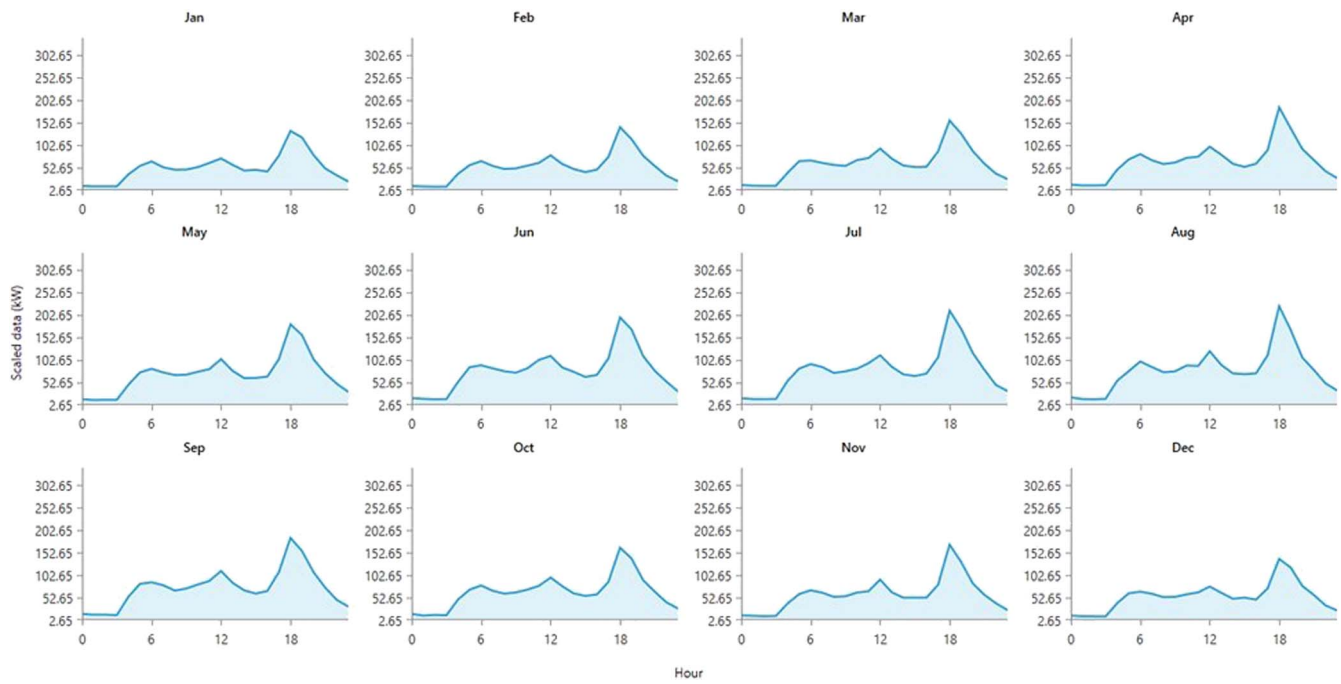$$P_{PV} = P_r . f_{PV} \left(\frac{G_T}{G_S} \right) [1 + \alpha_P (T_C - T_S)] \qquad (1)$$

Figure 6. Hourly distribution pattern for the specified area within Zhanjiang city.
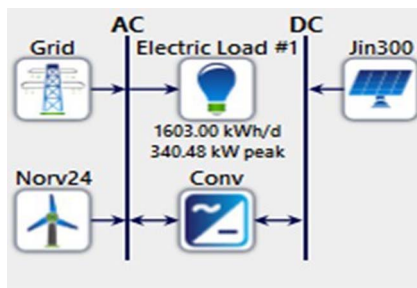

Figure 7. The grid-connected hybrid WT/PV configuration diagram

Table 2. Technical and financial information of the chosen PV modules [38]

Item	Specification
PV slope	22°
Azimuth	0°
Discount factor (DF)	85%
Cost of investment	$260
Cost of replacement	0
O&M expenses	$10/year/kW
Lifespan	25 years
Size	0–400 kW, 200 intervals

The rated capacity of the PV panels is designated as P_r (kW), with f_{pv} (%) representing the PV derating factor in percentage terms and G_T (kW/m^2) indicating the instantaneous sunlight irradiation on the PV panels during the time step in terms of kilowatts per square meter. G_S (1000 W/m^2) stands for instantaneous sunlight irradiation on PV panels under standard test conditions (STC). The term "α_p" represents the temperature coefficient of power, which is expressed as a percentage change per degree Celsius (°C). The temperature of solar panels in the STC (25°C) is represented by T_s, whereas the actual temperature of the PV panels is represented by T_C (°C).

The PV arrays are expected to have a construction cost of $260/kW, and the estimated operation and maintenance costs (O&M) costs are $10/kW. The PV arrays lack a tracking mechanism and are permanently positioned at a 22° slope and a 0° azimuth. Table 2 [38] provides detailed information about the unique attributes of the PV panels.

2.4.2 Wind turbine

The 100 kW WT (Norvento nED 24) has been chosen for evaluation in the current study. This WT stands at 36 m tall at the hub and has a rotor diameter of 24 m. Fig. 8 shows the

Figure 8. The Norvento nED 24 WT's power graph.

power efficiency of the Norvento nED 24. The WT's capacity is maximized by means of the HOMER optimizer. The WT's capacity is maximized by means of the HOMER optimizer. Moreover, Table 3 [39] provides comprehensive technical and financial details pertaining to the WT.

The level of electricity generated by a WT depends on the current density of the air. In order to calculate wind velocity at the hub elevation of a WT, it is necessary to employ the

Table 3. Information regarding the technical specifications and financial details of the Norvento nED 24 WT

Item	Specification
Diameter of the rotor	24 m
Hub elevation	36 m
Power rating	100 kW
Costs of capital	$150 000
Costs of replacement	$120 000
Operating and maintenance expenses	$500/year/kW
Lifespan	20 years
Quantity	1

Table 4. Information regarding the technical specifications and financial details of the converter

Item	Specification
Capital expenses	$890/kW
Replacement costs	$780/kW
Expenses of O&M	$10/year/kW
Lifespan	15 years
Efficiency	95%
Capacity	0–600 kW, 150 intervals

following equation [40]:

$$V_{hub} = V_a . \left(\frac{H_{hub}}{H_a}\right)^\alpha \tag{2}$$

The wind velocity at a specific height, denoted by H_{hub} and expressed in meters, is represented by V_{hub}, while the wind velocity at a different height, denoted by H_a and expressed in meters, is represented by V_a. The value of α (power-law coefficient) is influenced by a multitude of factors, including wind velocity, surface roughness, height, and other variables. In this analysis, we assume that the value of α is 0.14.

The power curve demonstrates the efficiency of a WT under normal atmospheric conditions. The predicted output power [$P_{ws}(V)$] of the Norvento nED 24 WT is determined using a mathematical model based on the following equation [41].

$$P_{WS}(V) = \begin{cases} 0, & 0 \ll V < V_C \\ P_R \frac{(V-V_C)}{(V_R-V_C)}, & V_C \ll V < V_R \\ P_R, & V_R \ll V \ll V_F \\ 0, & V > V_F \end{cases} \tag{3}$$

The variables included in the equation are as follows:

The wind velocity is represented by V, the cut-in wind velocity by V_c, the rated wind velocity by V_R, the furling wind velocity by V_F, and the rated power of the WT is represented by P_R (kW).

A common approach to analyzing the performance of WT is to use a power curve, which delineates the turbine's output under standard temperature and pressure (STP) conditions. The following formula [32] is utilized in order to determine the output power, denoted by $P_w(V)$, of the WT under the actual operational circumstances.

$$P_w(V) = \left(\frac{\rho}{rho_{stp}}\right) . P_{ws}(V) \tag{4}$$

Here, ρ represents the actual air density (kg/m³), while ρ_{stp} represents the air density at STP, which is 1.225 kg/m³.

2.4.3 Converter

Power converters are a crucial component of hybrid energy systems. Their function is to convert AC to DC [37]. The capacity requirements for inverters based on the flow of energy from a DC to an AC can be determined by the

following equation [42]:

$$eta_{inv} = \frac{P_i}{P_o} \tag{5}$$

P_i, the inverter's electrical power input, is determined exclusively by the inverter's input power. In a similar vein, the inverter's output electrical power, P_o, and its output power are exactly equal. It is anticipated that the converter will incur capital expenses amounting to $890, replacement costs totaling $780, and annual O&M expenses of $10/kW. It is anticipated that the converter will function for 15 years with an efficiency rate of 95%. The converter's effectiveness is enhanced using the HOMER optimizer. The converter now under examination is described in full in Table 4 [43].

2.5 Evaluation model

The net present cost (NPC) is determined by subtracting the current value of expenses from the current value of benefits received throughout the system's duration. By determining the reduction in the present value of all incoming and outgoing cash for each year throughout the project's timeline. HOMER assesses system configurations by comparing them using the NPC formula as described in reference [44]:

$$NPC = \frac{C_{tac}}{CRF(i, n)} \tag{6}$$

The formula for the capital recovery factor (CRF) is utilized in determining the total annualized cost of the system, known as C_{tac} ($/year), when applied to NPC [45].

$$CRF(i, n) = \frac{i(1+i)^n}{(1+i)^n - 1} \tag{7}$$

The formula uses n to indicate the project's lifespan in years and i to represent the yearly real interest rate (%). This analysis supposes that the project will have a duration of 25 years. The formula provided can be utilized to calculate the annual effective interest rate (i), which is connected to the nominal interest rate (i_{nom}) and the inflation rate (f_a) [46]:

$$i = \frac{i_{nom} - f_a}{1 + f_a} \tag{8}$$

The levelized cost of energy is determined by dividing the whole life cycle cost by the total lifetime energy production. HOMER employs the equation provided in reference [47] to

Table 5. Controls and restrictions in the software to manage system functions

Items	Value
Project lifetime	25 years
LF	Yes
Charge in cycles	Yes
Apply the set point	Yes
Constraints minimal percentage of renewables	35%
Maximum yearly capacity shortage percentage	2%
Load in current time step	10%
Peak load per year	2%
Energy produced by solar panels	80%
Energy generated by WTs	50%

calculate the COE.

$$COE = \frac{C_{tot}}{E_{pro}} \qquad (9)$$

The variable C_{tot} represents the overall annual cost of the system in dollars, while E_{pro} represents the entire electricity production over its lifetime in kilowatt-hours (kWh).

The project's 25-year lifetime is given in the report, along with nominal discount rates of 3.76% and 0.2% for inflation.

2.6 Model of the environment

Most of the greenhouse gas emissions in hybrid power generation systems come from diesel and other fuel-powered generators, along with the fuel used by traditional power networks [48]. This study specifically examines the ecological impacts of carbon dioxide emissions. The grid's CO_2 emissions can be computed using the formula specified in reference [49]:

$$M_e = 1000.F_e.E_g \qquad (10)$$

The equation represents the relationship between carbon dioxide emissions per year (M_e) measured in kilograms per year (kg/year), the emission factor for grid energy (E_g) measured in grams per kilowatt-hour (g/kWh), and the yearly quantity of electricity purchased from grid power (F_e) measured in kilowatt-hours per year.

The computation of the renewable fraction (RF) involves dividing the total electricity produced by the power system by the amount of electricity derived from renewable energy sources [50].

$$RF = \left(\frac{E_{ren}}{E_{ren} + E_{non-ren}} \right) 100\% \qquad (11)$$

E_{ren} symbolizes the amount of kilowatt-hour produced by renewable energy sources annually. On the other hand,

$E_{non-ren}$ indicates the amount of electricity produced (kWh) from nonrenewable energy sources during the same time-frame.

2.7 Constraints

HOMER enhances performance through the utilization of dispatch methods, search space amounts, and sensitivity range parameters. Capacity shortages do not incur any penalties. Information on the system that manages the settings utilized in the simulation's execution restrictions can be found in Table 5.

2.8 Single and multiyears modules

The HOMER software's 1-year edition uses a grid search algorithm and a specialized derivative-free method to model the exploration area and adjust system component sizes. This is achieved through a process of exhaustive search, whereby the entire search space is exhaustively explored, and the optimal solution is identified through a process of minimizing the cost function [51]. The multiyear module is specifically designed to replicate the progress that occurs throughout the whole course of a project. Throughout the project's life cycle, HOMER is used to reproduce every year. The present study estimates a 0.5% annual rise in the electric load and a 0.5% decline in PV efficiency. Additionally, it is expected that the system's fixed operation and maintenance expenses will remain constant throughout time [52].

3 Results and discussion

This article examines the potential for integrating renewable energies into China's regions rich in their natural resources. The HOMER Pro software is utilized to design, examine, and evaluate a hybrid power configuration for a fictitious small district consisting of 100 dwellings in Zhanjiang.

3.1 Optimization results

The outcomes of optimizing hybrid power systems with the multiyear module are shown in Table 6. The small district of Zhanjiang city has three feasible choices for energy systems: PV–WT–grid, WT–grid, and PV–grid. The most economically efficient choice is the 80 kW PV–WT–grid hybrid system with the load following (LF) approach, consisting of one WT and 25.55 kW converters. This option has a total NPC of \$494 119 and a COE of \$0.043/kWh. Nevertheless, the PV–grid configuration was considered uneconomical due to its high NPC of \$687 906 and COE of \$0.068/kWh. The predicted annual carbon dioxide emissions for the optimal PV–wind–grid system are 174 236 kg/year, while the PV–grid configuration, serving as the baseline configuration under the LF strategy, has the highest annual carbon dioxide emissions of 246 769 kg/year. Furthermore, within the PV–grid system,

Table 6. The hybrid system's technical and economic characteristics

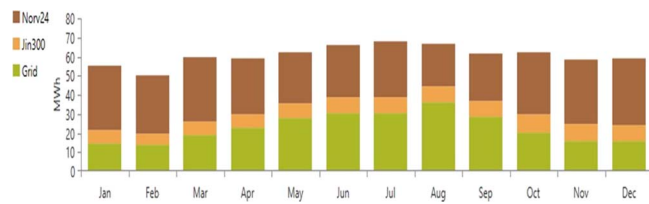| Configuration	PV (kW)	WT (quantity)	Converter (kW)	Dispatch	COE ($/kWh)	NPC ($)	OC ($/year)	IC ($)	RF (%)	Excess electricity (%)	CO_2 (kg/year)
WT/PV/grid	80	1	25.55	LF	0.043	494 119	18 339	193 591	60.67	3.16	174 236
Grid/WT		1		LF	0.045	495 597	21 089	150 000	53.18	0	198 979
Grid/PV	267.33		85.17	LF	0.068	687 906	33 111	145 305	36.60	10.88	246 769

Figure 9. Electricity generation of every unit within the ideal PV–WT–grid system.

Table 7. Optimal setup for electricity generation and utilization using PV/WT/DG/battery

| Component	Production	Percentage
Jinko Solar300JKM300M-72	94 155 kWh/year	12.9
Norvento nED 24 [100 kW]	357 694 kWh/year	49.2
Grid purchases	275 689 kWh/year	37.9
Total	727 538 kWh/year	100
Component	**Consumption**	**Percentage**
AC primary load	585 095 kWh/year	83.5
DC primary load	0	0
Deferrable load	0	0
Sales grid	115 889 kWh/year	16.5
Total	700 984 kWh/year	100
Quantity	**Value**	
Excess electricity	22 996 kWh/year	
Unmet electric load	0	
Lack of capacity	0	
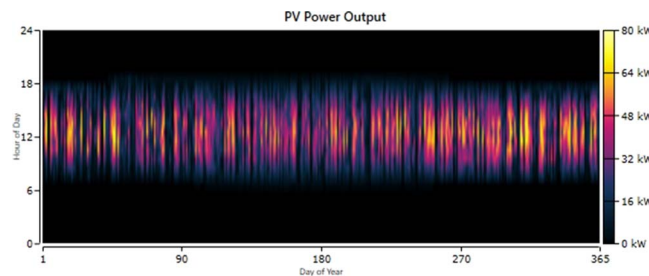
Figure 10. Output of power the PV.

the absence of a WT led to a higher NPC, and the hybrid system required extensive space for the installation of its solar panels. The hybrid arrangement of WT, PV, and grid is thought to be the most economical and ecologically sustainable choice.

In Fig. 9, the electricity generation of every part in the ideal WT–PV–grid hybrid configuration is displayed for each month during the initial year. The residential buildings examined showed that most of their electricity comes from WT power generation, specifically 357 694 kWh/year, making up roughly 49.2% of the total power produced. Subsequently, the majority of their energy is derived from grid power generation and PV power generation, with an annual output of 275 689 and 94 155 kWh, respectively. These sources contribute 37.9% and 12.9% of the overall power generation, respectively.

Table 7 presents the power output of each component in the ideal PV–WT–grid configuration. The surplus electrical energy generated by this highly efficient system amounts to 22 996 kWh each year, which accounts for 3.16% of the total production. Additionally, there is no underutilized capacity or unmet demand. Figs 10 and 11 depict the generating patterns of the solar panels and WT power.
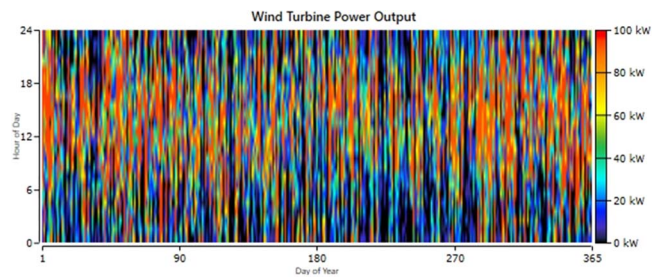

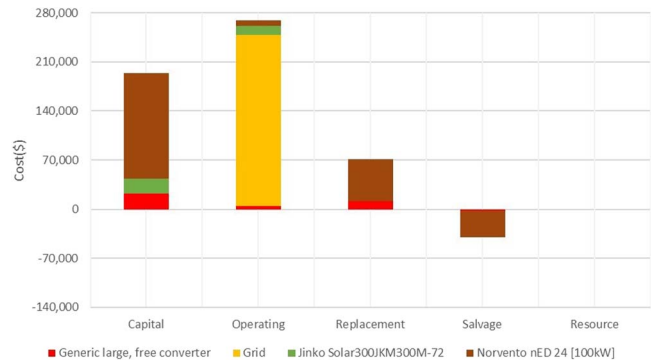Figure 11. Output of power the WT.

Figure 12. The cost breakdown summary of capital, salvage, replacement, and O&M expenses for the most efficient WT–PV–grid configuration.

3.2 Economic analysis results

Fig. 12 offers a detailed visual representation of the overall costs, including capital, O&M, replacement, and salvage expenses linked to the ideal PV–WT–grid configuration. The grid has the highest NPC of $243 880 due to its elevated operational and maintenance (O&M) expenses. On the other hand, the PV has the smallest NPC at $33 995. The Norvento nED 24 WT shows the biggest first investment and most expensive repair expenses. As a result, cutting costs related to the grid and the Norvento nED 24 WT could effectively lower the overall system expenses.

Fig. 13a and b presents a comparison of cash flow outcomes in nominal terms between the optimal WT–PV–grid configuration and the base PV–grid configuration across the entire lifespan of the project. The PV–WT–grid configuration offers a greater number of advantages in terms of cost savings and recovery compared to the PV–grid configuration. It is evident that this demonstrates the economic viability of the PV–WT–grid configuration over the entire 25-year project lifespan.

Fig. 14 shows the total cash flows of the current configuration and the proposed configuration for a period of 25 years. It also shows the important point where the two configurations that decide the length of time it takes to receive a discount intersect. The PV–grid configuration is compared to the PV–WT–grid hybrid configuration, with a calculated discount payback period of 3 years.

3.3 Environmental performance analysis

Table 8 provides a detailed examination of the environmental effects of key pollutants (such as CO_2, carbon monoxide, SO_2, and NOx) released by various systems. It is noteworthy that carbon dioxide emissions are the most prominent. The PV–WT–grid hybrid system, which does not release any emissions,
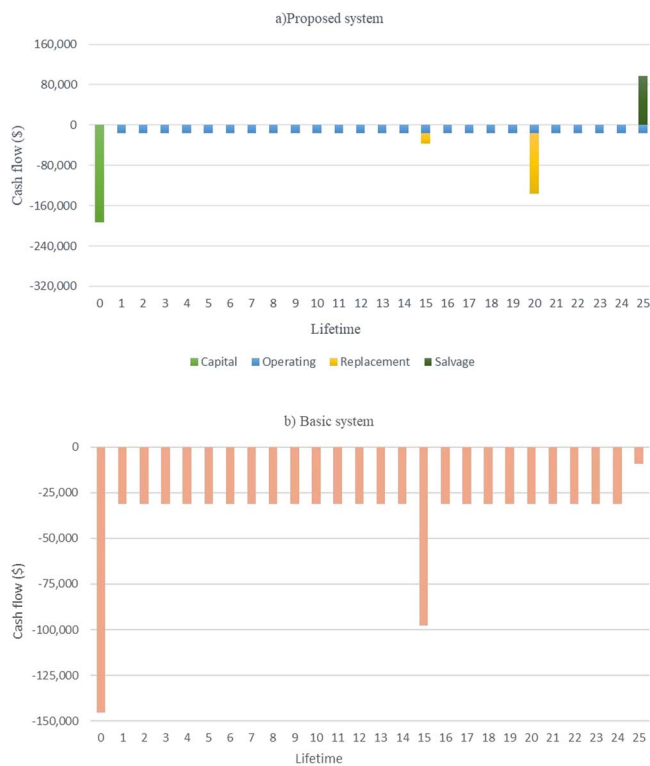
Figure 13. An evaluation of the yearly monetary income difference between the ideal setup (a) and the basic system (b).
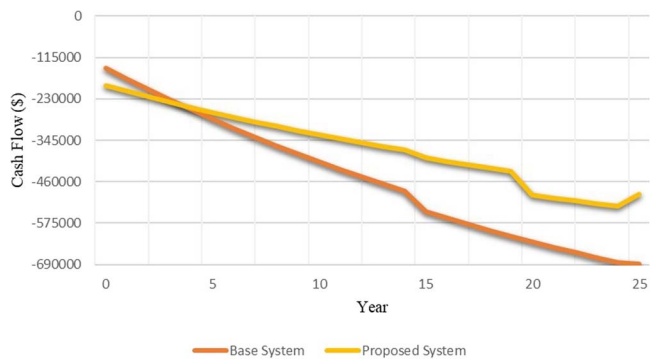

Figure 14. Comparison between the total cash flow of the WT–PV–grid hybrid configuration and the base configuration.

is the most environmentally friendly option. Conversely, the PV–grid hybrid system, which emits the greatest quantity of CO_2 (246 769 kg/year), emerges as the most polluting among the systems analyzed.

3.4 Sensitivity analysis

Fig. 15 depicts the NPC value of the optimal systems as wind velocity or solar irradiation data (sensitivity variables) are modified. The optimal system is depicted on the graphical surface with the NPC overlaying it. The optimal system's NPC value is inversely proportional to the wind speed or solar irradiation value. In other words, an increase in wind velocity or solar irradiation can enhance the economic system. Moreover, the figure demonstrates how the optimal system type varies based on different wind velocity or solar irradiation values. The WT–PV–grid configuration is likely to be the optimal choice when the wind velocity is below 5.76 m/s. When wind

Table 8. Emissions are released from every conceivable system

Pollutant	Quantity (kg/year)
CO_2	174 236
CO	0
Unburned hydrocarbon	0
Particulate matter	0
SO_2	755
NO_2	369

velocity exceeds 5.76 m/s within the current solar irradiation range, the WT–grid system may be the optimal choice.

Fig. 16 presents a graphical illustration of the fluctuation of COE and NPC values in response to varying nominal discount rates and wind speeds. The NPC is represented by a graphical surface, with the COE superimposed on top. At the current nominal discount rates, the most efficient configuration is the PV–WT–grid system. When the discount rate goes up from 3.5% to 4.25%, the NPC value of the best system decreases and its COE value increases. This indicates that the selection of an appropriate nominal discount rate is of paramount importance for the economic viability of the system. Furthermore, an increase in wind velocity from 5.4 to 6.3 m/s results in a reduction in both the NPC and COE values of the optimal configuration.

The findings indicate that surplus energy levels are directly impacted by solar irradiation and wind velocity, as shown in Fig. 17. The visual depiction shows the excess electricity, with the COE displayed on top. An increase in yearly average sunlight intensity from 3.6 to 4.5 kWh/m²/day causes surplus electricity to grow and COE to drop. Likewise, a rise in wind velocity from 5.4 to 6.3 m/s leads to a reduction in both excess electricity and COE.

3.5 Policy implications

An alternative energy system combining WT power has the potential to be a viable option for Zhanjiang city in China due to the city's abundance of wind resources, particularly in urban areas. With the requisite funding or government support, these systems could provide a sustainable and environmentally friendly option for urban electrification in China and other developing countries. Research needs to consider various factors such as fuel limitations, resale value, excess electricity management, potential adjustments to project duration, and energy consumption to create dependable and affordable standalone hybrid energy systems. Future research should also examine the impact of different control methods on hybrid systems with multiple fuel types. Moreover, future studies will investigate the potential for hybrid energy systems combining biomass power generation with other renewable sources to enhance their efficacy and cost-effectiveness.

4 Conclusions

This study extensively examines a hybrid grid-connected power configuration, considering environmental, technological, and economic factors to identify the most effective approach for meeting the energy needs of a small community. The research utilized HOMER software to optimize the design of hybrid energy configurations for a cluster of 100 homes in Zhanjiang City, situated in Guangdong Province, China. Furthermore, various sensitivity analyses were conducted in
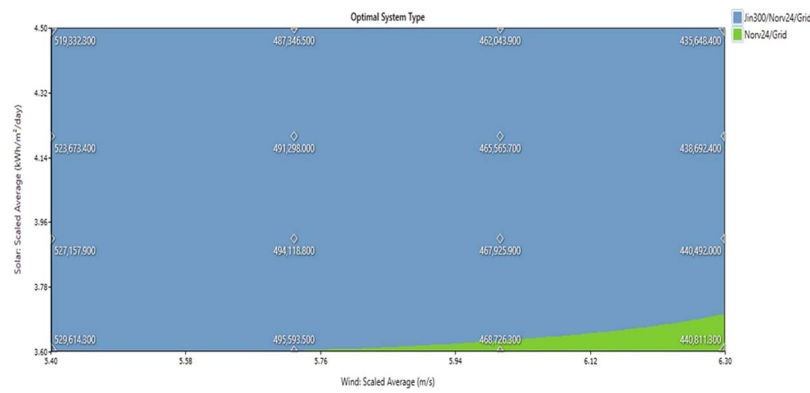
Figure 15. Analyzing data on wind velocity and solar irradiation determines the best system type.
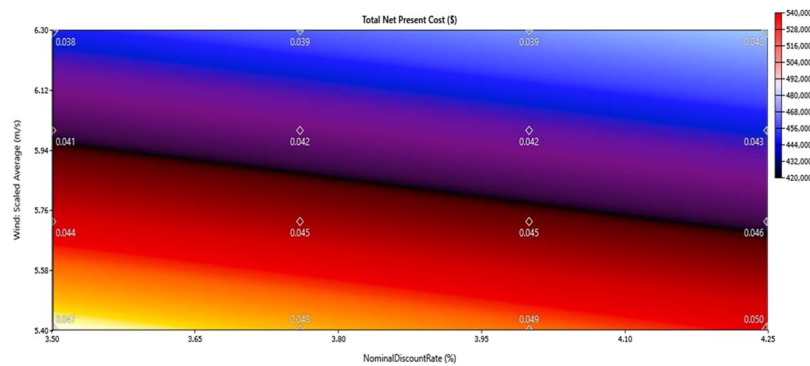

Figure 16. The influence of alterations in both the nominal discount rate and wind velocity on the system's NPC and COE.
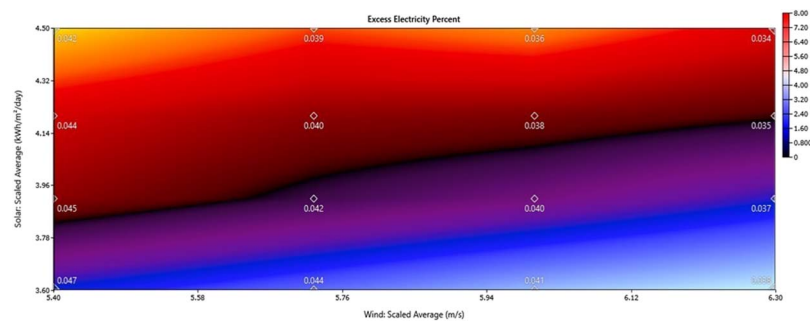

Figure 17. Variations in solar irradiation and wind velocity impact the excess of power and carbon dioxide emissions.

the study to ascertain the impact of different input parameters, such as the discount rate, solar irradiation level, and wind velocity, on the ideal hybrid configuration. In summary, the key results of this investigation are outlined as follows:

The findings indicate that the most economical WT–PV–grid hybrid setup with the LF approach includes 80 kW of PV panels, a single WT, and 25.55 kW of converters. This specific system shows a total NPC of \$494 119 and a COE of \$0.043/kWh. The optimal system generates an excess of 22 996 kWh/year (3.16%), with no unmet demand or capacity shortfall. Conversely, the PV–grid hybrid system exhibits the highest NPC (\$687 906) and COE (\$0.068/kWh), attributable to the highest operational costs. In the PV–grid configuration, the absence of a WT resulted in an increase in the NPC, while the hybrid configuration's solar panel installation necessitated a considerable amount of space. The most cost-effective and environmentally friendly choice is the PV–WT–grid hybrid configuration. Moreover, results of the multiyear system's performance assessment indicate that the majority of electricity

consumed in residential structures was generated by WTs. This accounted for a total of 357 694 kWh/y, representing approximately 49.2% of the overall electricity produced. Following that, the residential buildings being analyzed mainly receive electricity from grid power and solar power, producing 275 689 and 94 155 kWh/year, respectively. These amounts represent 37.9% and 12.9% of the total power generated. The suggested PV–WT–grid configuration, which is considered the best option, has an annual CO_2 emission of 174 236 kg/year. On the other hand, the PV–grid system, functioning as the foundation system in the LF strategy, is responsible for emitting 246 769 kg/year of CO_2 annually.

The findings from the sensitivity analysis indicate that as solar radiation increases without any change in wind speed, the COE and NPC of the optimal system decrease. In addition, the ideal system's COE and NPC values decrease as wind velocity increases, with solar irradiation remaining constant. Enhancing either the wind speed or solar radiation level can boost the economic efficiency of the system. Moreover,

the picture suggests that the best system type could change based on wind speed or levels of solar radiation. A PV–WT–grid system is likely the most effective if wind speed drops below 5.76 m/s. If the wind speed exceeds 5.76 m/s, the WT–grid system is recommended within the current solar irradiation range. The best choice is the PV–WT–grid setup due to the current nominal discount rate. The NPC value of the optimal setup decreases when the nominal discount rate rises from 3.5% to 4.25%, but the equity value cost increases. Hence, choosing the right nominal discount rate is advised to guarantee the financial sustainability of the system. The results indicate that excess energy levels are directly influenced by solar irradiation and wind velocity. An increase in the yearly average irradiation level from 3.6 to 4.5 kWh/m^2/day resulted in a higher surplus electricity percentage and a lower equity cost. Additionally, an increase in wind speed from 5.4 to 6.3 m/s resulted in a reduction in both the surplus electricity percentage and the COE.

In general, it is important to recognize that cities such as Zhanjiang have the capability to adopt hybrid renewable energy systems, and the economic and environmental justification for investing in PV–WT–grid and WT–grid systems could be seen in the coming years. Given enough financial backing or assistance from the government, these systems could offer a sustainable and environmentally friendly solution for urban electricity needs in China and other emerging nations.

Acknowledgements

Author contributions

Tao Hai (Software [equal], Validation [equal], Writing—review & editing [equal]), Hussein Jaffar (Conceptualization [equal], Methodology [equal], Project administration [equal], Writing—original draft [equal]), Hayder Shami (Formal analysis [equal], Software [equal], Writing—original draft [equal]), Ameer Al-Rubaye (Data curation [equal], Formal analysis [equal], Supervision [equal], Visualization [equal]), Husam Rajab (Formal analysis [equal], Validation [equal], Writing—review & editing [equal]), Rand Farqad (Formal analysis [equal], Methodology [equal], Supervision [equal], Writing—review & editing [equal]), Abbas Abdul Hussein (Conceptualization [equal], Resources [equal], Software [equal], Writing—review & editing [equal]), Wesam Abed Alhaidry (Formal analysis [equal], Methodology [equal], Resources [equal], Writing—review & editing [equal]), Ameer Idan (Data curation [equal], Formal analysis [equal], Validation [equal], Writing—original draft [equal]), and Narinderjit Sawaran Singh (Formal analysis [equal], Software [equal], Visualization [equal], Writing—review & editing [equal]).

References

1. Li W, Yi P, Zhang D. *et al*. Assessment of coordinated development between social economy and ecological environment: case study of resource-based cities in northeastern China. *Sustain Cities Soc* 2020;59:102208. https://doi.org/10.1016/j.scs.2020.102208.
2. Zhu C, Zhang Y, Wang M. *et al*. Simulation and comprehensive study of a new trigeneration process combined with a gas turbine cycle, involving transcritical and supercritical CO2 power cycles and Goswami cycle. *J Therm Anal Calorim* 2024;149:6361–84. https://doi.org/10.1007/s10973-024-13182-9.
3. Li J, Chen S, Wu Y. *et al*. How to make better use of intermittent and variable energy? A review of wind and photovoltaic power consumption in China. *Renew Sustain Energy Rev* 2021;137:110626. https://doi.org/10.1016/j.rser.2020.110626.
4. Li B, Wang J, Nassani AA. *et al*. The future of green energy: a panel study on the role of renewable resources in the transition to a green economy. *Energy Econ* 2023;127:107026. https://doi.org/10.1016/j.eneco.2023.107026.
5. Feng Y, Chen J, Luo J. Life cycle cost analysis of power generation from underground coal gasification with carbon capture and storage (CCS) to measure the economic feasibility. *Resour Policy* 2024;92:104996. https://doi.org/10.1016/j.resourpol.2024.104996.
6. Chen G, Kuang R, Li W. *et al*. Numerical study on efficiency and robustness of wave energy converter-power take-off system for compressed air energy storage. *Renew Energy* 2024;232:121080. https://doi.org/10.1016/j.renene.2024.121080.
7. Wen D, Aziz M. Flexible operation strategy of an integrated renewable multi-generation system for electricity, hydrogen, ammonia, and heating. *Energ Conver Manage* 2022;253:115166. https://doi.org/10.1016/j.enconman.2021.115166.
8. Zhang J, Zhong A, Huang G. *et al*. Enhanced efficiency with CDCA co-adsorption for dye-sensitized solar cells based on metal-losalophen complexes. *Sol Energy* 2020;209:316–24. https://doi.org/10.1016/j.solener.2020.08.096.
9. Zafar U, Ur Rashid T, Khosa AA. *et al*. An overview of implemented renewable energy policy of Pakistan. *Renew Sustain Energy Rev* 2018;82:654–65. https://doi.org/10.1016/j.rser.2017.09.034.
10. Hai T, Jaffar HA, Taher HH. *et al*. Techno-economic and environmental analysis of a grid-connected rooftop solar photovoltaic system in three climate zones. *Int J Low-Carbon Technol* 2024;19:1725–39. https://doi.org/10.1093/ijlct/ctae123.
11. Kumar R, Agarwala A. Renewable energy technology diffusion model for techno-economics feasibility. *Renew Sustain Energy Rev* 2016;54:1515–24. https://doi.org/10.1016/j.rser.2015.10.109.
12. Duan Y, Zhao Y, Hu J. An initialization-free distributed algorithm for dynamic economic dispatch problems in microgrid: modeling, optimization and analysis. *Sustain Energy Grids Netw* 2023;34:101004. https://doi.org/10.1016/j.segan.2023.101004.
13. Kobayakawa T, Kandpal TC. Optimal resource integration in a decentralized renewable energy system: assessment of the existing system and simulation for its expansion. *Energy Sustain Dev* 2016;34:20–9. https://doi.org/10.1016/j.esd.2016.06.006.
14. Li C, Zhou D, Zhang L. *et al*. Exploration on the feasibility of hybrid renewable energy generation in resource-based areas of China: case study of a regeneration city. *Energ Strat Rev* 2022;42:100869. https://doi.org/10.1016/j.esr.2022.100869.
15. Das BK, Zaman F. Performance analysis of a PV/diesel hybrid system for a remote area in Bangladesh: effects of dispatch strategies, batteries, and generator selection. *Energy* 2019;169:263–76. https://doi.org/10.1016/j.energy.2018.12.014.
16. Rad MAV, Shahsavari A, Rajaee F. *et al*. Techno-economic assessment of a hybrid system for energy supply in the affected areas by natural disasters: a case study. *Energ Conver Manage* 2020;221:113170. https://doi.org/10.1016/j.enconman.2020.113170.
17. Singh A, Baredar P. Techno-economic assessment of a solar PV, fuel cell, and biomass gasifier hybrid energy system. *Energy Rep* 2016;2:254–60. https://doi.org/10.1016/j.egyr.2016.10.001.
18. Alsagri AS, Alrobaian AA, Nejlaoui M. Techno-economic evaluation of an off-grid health clinic considering the current and future energy challenges: a rural case study. *Renew Energy* 2021;169:34–52. https://doi.org/10.1016/j.renene.2021.01.017.
19. Isa NM, Das HS, Tan CW. *et al*. A techno-economic assessment of a combined heat and power photovoltaic/fuel cell/battery energy system in Malaysia hospital. *Energy* 2016;112:75–90. https://doi.org/10.1016/j.energy.2016.06.056.
20. Shezan SA, Fatin Ishraque M, Muyeen SM. *et al*. Effective dispatch strategies assortment according to the effect of the operation for an islanded hybrid microgrid. *Energ Conver Manage* 2022;14:100192. https://doi.org/10.1016/j.ecmx.2022.100192.
21. Ramesh M, Saini RP. Dispatch strategies based performance analysis of a hybrid renewable energy system for a remote rural area

in India. *J Clean Prod* 2020;**259**:120697. https://doi.org/10.1016/j.jclepro.2020.120697.

22. Chaurasia R, Gairola S, Pal Y. Technical, economic, and environmental performance comparison analysis of a hybrid renewable energy system based on power dispatch strategies. *Sustain Energy Technol Assess* 2022;**53**:102787. https://doi.org/10.1016/j.seta.2022.102787.

23. Kushwaha PK, Bhattacharjee C. Integrated techno-economic-enviro-socio design of the hybrid renewable energy system with suitable dispatch strategy for domestic and telecommunication load across India. *J Energy Storage* 2022;**55**:105340. https://doi.org/10.1016/j.est.2022.105340.

24. Akhtari MR, Baneshi M. Techno-economic assessment and optimization of a hybrid renewable co-supply of electricity, heat and hydrogen system to enhance performance by recovering excess electricity for a large energy consumer. *Energ Conver Manage* 2019;**188**:131–41. https://doi.org/10.1016/j.enconman.2019.03.067.

25. Ramli MAM, Hiendro A, Twaha S. Economic analysis of PV/diesel hybrid system with flywheel energy storage. *Renew Energy* 2015;**78**:398–405. https://doi.org/10.1016/j.renene.2015.01.026.

26. Mousavi SA, Zarchi RA, Astaraei FR. *et al.* Decision-making between renewable energy configurations and grid extension to simultaneously supply electrical power and fresh water in remote villages for five different climate zones. *J Clean Prod* 2021;**279**:123617. https://doi.org/10.1016/j.jclepro.2020.123617.

27. Maleki Tehrani M, Akhtari M, Kasaeian A. *et al.* Techno-economic investigation of a hybrid biomass renewable energy system to achieve the goals of SDG-17 in deprived areas of Iran. *Energ Conver Manage* 2023;**291**:117319. https://doi.org/10.1016/j.enconman.2023.117319.

28. Tiam Kapen P, Medjo Nouadje BA, Chegnimonhan V. *et al.* Techno-economic feasibility of a PV/battery/fuel cell/electrolyzer/biogas hybrid system for energy and hydrogen production in the far north region of Cameroon by using HOMER pro. *Energ Strat Rev* 2022;**44**:100988. https://doi.org/10.1016/j.esr.2022.100988.

29. Toopshekan A, Yousefi H, Astaraei FR. Technical, economic, and performance analysis of a hybrid energy system using a novel dispatch strategy. *Energy* 2020;**213**:118850. https://doi.org/10.1016/j.energy.2020.118850.

30. Zamanpour K, Vaziri Rad MA, Saberi N. *et al.* Techno-economic comparison of dispatch strategies for stand-alone industrial demand integrated with fossil and renewable energy resources. *Energy Rep* 2023;**10**:2962–81. https://doi.org/10.1016/j.egyr.2023.09.095.

31. He L, Zhang S, Chen Y. *et al.* Techno-economic potential of a renewable energy-based microgrid system for a sustainable large-scale residential community in Beijing, China. *Renew Sustain Energy Rev* 2018;**93**:631–41. https://doi.org/10.1016/j.rser.2018.05.053.

32. Dhundhara S, Verma YP, Williams A. Techno-economic analysis of the lithium-ion and lead-acid battery in microgrid systems. *Energ Conver Manage* 2018;**177**:122–42. https://doi.org/10.1016/j.enconman.2018.09.030.

33. Ahmed MM, Das BK, Das P. *et al.* Energy management and sizing of a stand-alone hybrid renewable energy system for community electricity, fresh water, and cooking gas demands of a remote island. *Energ Conver Manage* 2024;**299**:117865. https://doi.org/10.1016/j.enconman.2023.117865.

34. Li C, Zhou D, Wang H. *et al.* Feasibility assessment of a hybrid PV/diesel/battery power system for a housing estate in the severe cold zone—a case study of Harbin, China. *Energy* 2019;**185**:671–81. https://doi.org/10.1016/j.energy.2019.07.079.

35. "Zhanjiang," Mapcarta. Accessed: Apr. 28, 2024. https://mapcarta.com/Zhanjiang

36. Li C, Zheng Y, Li Z. *et al.* Techno-economic and environmental evaluation of grid-connected and off-grid hybrid intermittent power generation systems: a case study of a mild humid subtropical climate zone in China. *Energy* 2021;**230**:120728. https://doi.org/10.1016/j.energy.2021.120728.

37. El-houari H, Allouhi A, Salameh T. *et al.* Energy, economic, environment (3E) analysis of WT–PV–battery autonomous hybrid power plants in climatically varying regions. *Sustain Energy Technol Assess* 2021;**43**:100961. https://doi.org/10.1016/j.seta.2020.100961.

38. Li C, Zhang L, Qiu F. *et al.* Optimization and enviro-economic assessment of hybrid sustainable energy systems: the case study of a photovoltaic/biogas/diesel/battery system in Xuzhou, China. *Energ Strat Rev* 2022;**41**:100852. https://doi.org/10.1016/j.esr.2022.100852.

39. Rehman S, Natrajan N, Mohandes M. *et al.* Feasibility study of hybrid power systems for remote dwellings in Tamil Nadu, India. *IEEE Access* 2020;**8**:143881–90. https://doi.org/10.1109/ACCESS.2020.3014164.

40. Sharma R, Kodamana H, Ramteke M. Multi-objective dynamic optimization of hybrid renewable energy systems. *Chem Eng Process - Process Intensif* 2022;**170**:108663. https://doi.org/10.1016/j.cep.2021.108663.

41. Medina JP, Lata-García J. Optimal model of a hybrid electrical system photovoltaic panel /wind turbine/battery bank, considering the feasibility of implementation in isolated areas. *J Energy Storage* 2021;**36**:102368. https://doi.org/10.1016/j.est.2021.102368.

42. Das BK, Hasan M, Rashid F. Optimal sizing of a grid-independent PV/diesel/pump-hydro hybrid system: a case study in Bangladesh. *Sustain Energy Technol Assess* 2021;**44**:100997. https://doi.org/10.1016/j.seta.2021.100997.

43. Halabi LM, Mekhilef S. Flexible hybrid renewable energy system design for a typical remote village located in tropical climate. *J Clean Prod* 2018;**177**:908–24. https://doi.org/10.1016/j.jclepro.2017.12.248.

44. Amutha WM, Rajini V. Cost benefit and technical analysis of rural electrification alternatives in southern India using HOMER. *Renew Sustain Energy Rev* 2016;**62**:236–46. https://doi.org/10.1016/j.rser.2016.04.042.

45. Mandal S, Das BK, Hoque N. Optimum sizing of a stand-alone hybrid energy system for rural electrification in Bangladesh. *J Clean Prod* 2018;**200**:12–27. https://doi.org/10.1016/j.jclepro.2018.07.257.

46. Li C, Zhou D, Zheng Y. Techno-economic comparative study of grid-connected PV power systems in five climate zones, China. *Energy* 2018;**165**:1352–69. https://doi.org/10.1016/j.energy.2018.10.062.

47. Padrón I, Avila D, Marichal GN. *et al.* Assessment of hybrid renewable energy systems to supplied energy to autonomous desalination systems in two islands of the canary archipelago. *Renew Sustain Energy Rev* 2019;**101**:221–30. https://doi.org/10.1016/j.rser.2018.11.009.

48. Zhu C, Zhang Y, Wang M. *et al.* Optimization, validation and analyses of a hybrid PV–battery–diesel power system using enhanced electromagnetic field optimization algorithm and ε-constraint. *Energy Rep* 2024;**11**:5335–49. https://doi.org/10.1016/j.egyr.2024.04.043.

49. Ma WW, Rasul MG, Liu G. *et al.* Climate change impacts on techno-economic performance of roof PV solar system in Australia. *Renew Energy* 2016;**88**:430–8. https://doi.org/10.1016/j.renene.2015.11.048.

50. Olatomiwa L, Mekhilef S, Huda ASN. *et al.* Economic evaluation of hybrid energy systems for rural electrification in six geo-political zones of Nigeria. *Renew Energy* 2015;**83**:435–46. https://doi.org/10.1016/j.renene.2015.04.057.

51. Baruah A, Basu M, Amuley D. Modeling of an autonomous hybrid renewable energy system for electrification of a township: a case study for Sikkim, India. *Renew Sustain Energy Rev* 2021;**135**:110158. https://doi.org/10.1016/j.rser.2020.110158.

52. Aziz AS, Tajuddin MFN, Adzman MR. *et al.* Optimization and sensitivity analysis of standalone hybrid energy systems for rural electrification: a case study of Iraq. *Renew Energy* 2019;**138**:775–92. https://doi.org/10.1016/j.renene.2019.02.004.